

Supplementary information

High-throughput “read-on-ski” automated imaging and label-free detection system for toxicity screening of compounds using personalised human kidney organoids

Qizheng WANG¹, Jun LU^{2,3}, Ke FAN², Yiwei XU², Yucui XIONG², Zhiyong SUN^{2,3}, Man ZHAI², Zhizhong ZHANG^{2,3}, Sheng ZHANG², Yan SONG², Jianzhong LUO², Mingliang YOU⁴, Meijin GUO¹, Xiao ZHANG^{2,3}

¹State Key Laboratory of Bioreactor Engineering, East China University of Science and Technology, Shanghai 200237, China

²Guangzhou Institutes of Biomedicine and Health, Chinese Academy of Sciences, Guangzhou 510530, China

³Bioland Laboratory (Guangzhou Regenerative Medicine and Health Guangdong Laboratory), Guangzhou 510320, China

⁴Hangzhou Cancer Institute, Key Laboratory of Clinical Cancer Pharmacology and Toxicology Research of Zhejiang Province, Affiliated Hangzhou Cancer Hospital, Zhejiang University School of Medicine, Hangzhou 310002, China

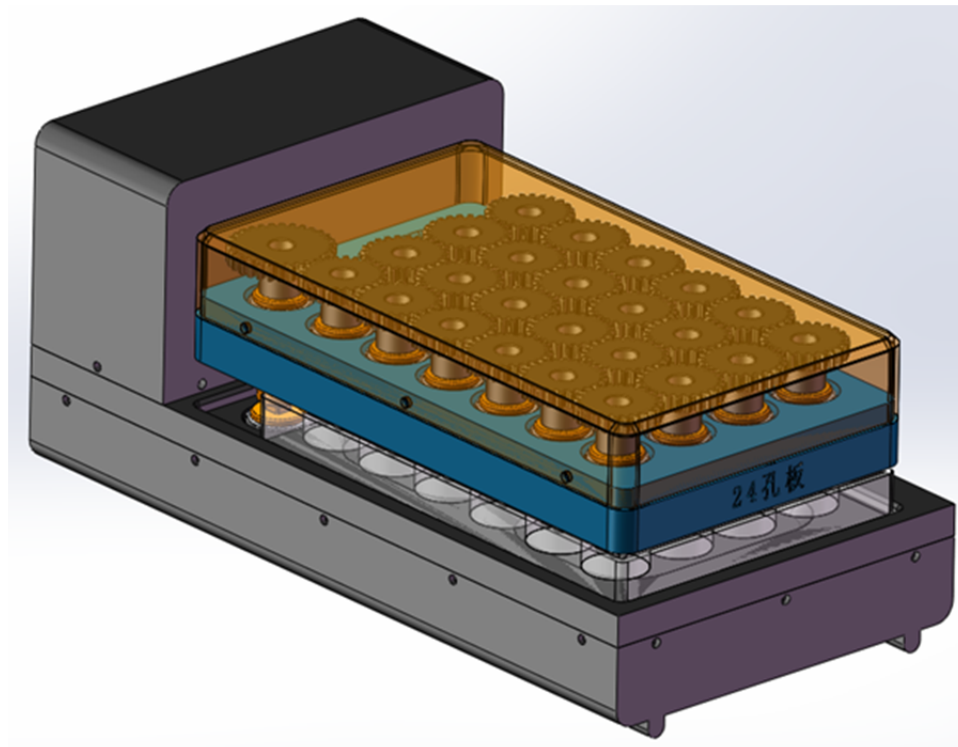


Fig. S1 Multi-well spin device implemented for generating kidney organoids in a batch format. The spin device can operate with 24/48-well plates with the master spin motor and interlinked with multiple stirring impellers.

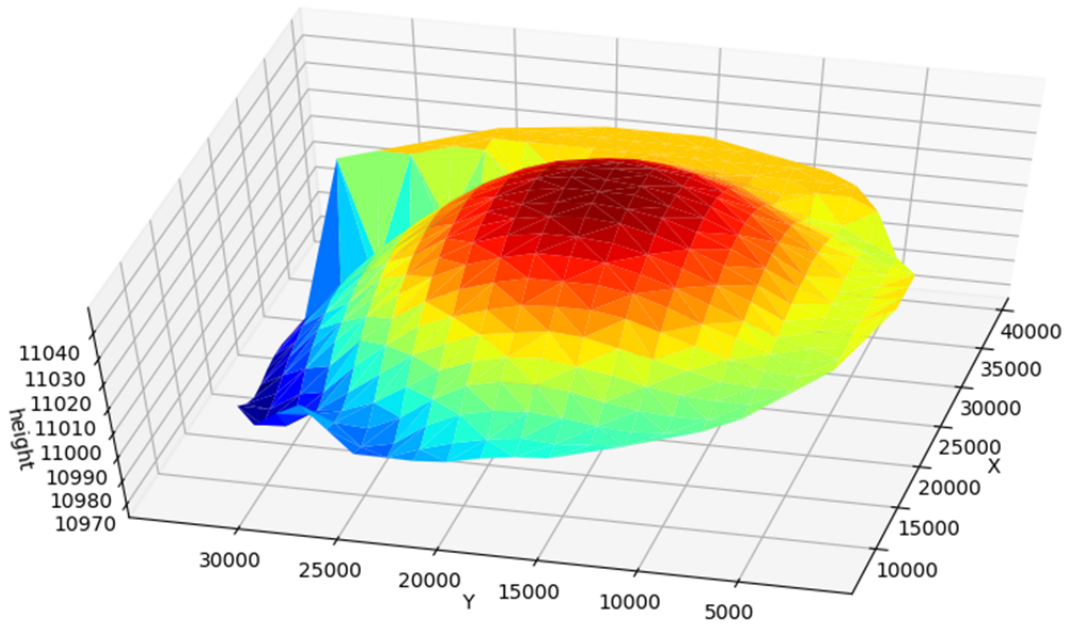


Fig. S2 Example of laser-based measurement for multi-well bottom surface (unit: μm). The scanning map for the height heat map shows that the uneven shape of the bottom has different focal planes for different areas. Based on this heat map, the pre-arranged Z-axis lens movement will implement non-stop movement in the autofocus system called “read-on-ski”.

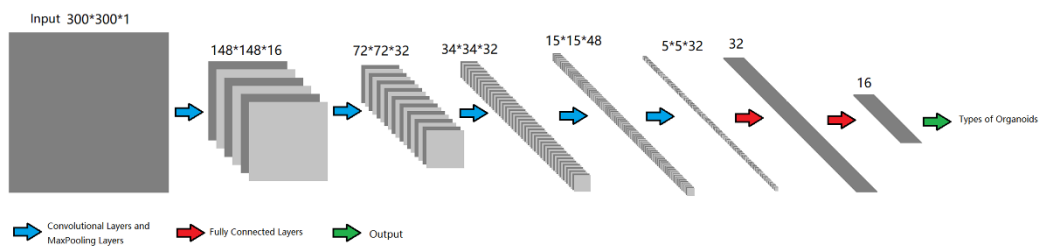


Fig. S3 Neural network architecture for the classification of organoids.

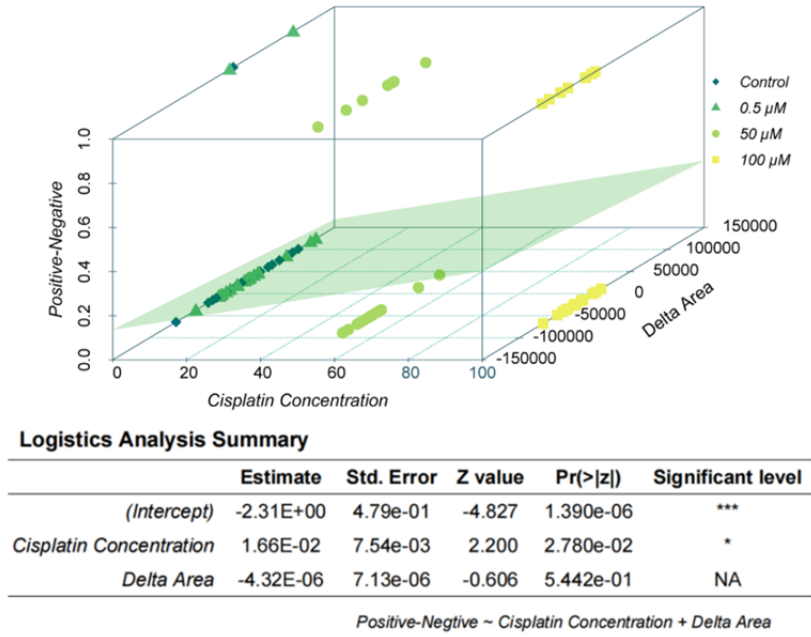


Fig. S4 Multiple logistic regression analysis. Prediction of treatment outcomes based on cisplatin concentrations and delta area using data from 96-well plate-based experiments. * $P < 0.05$, *** $P < 0.001$.

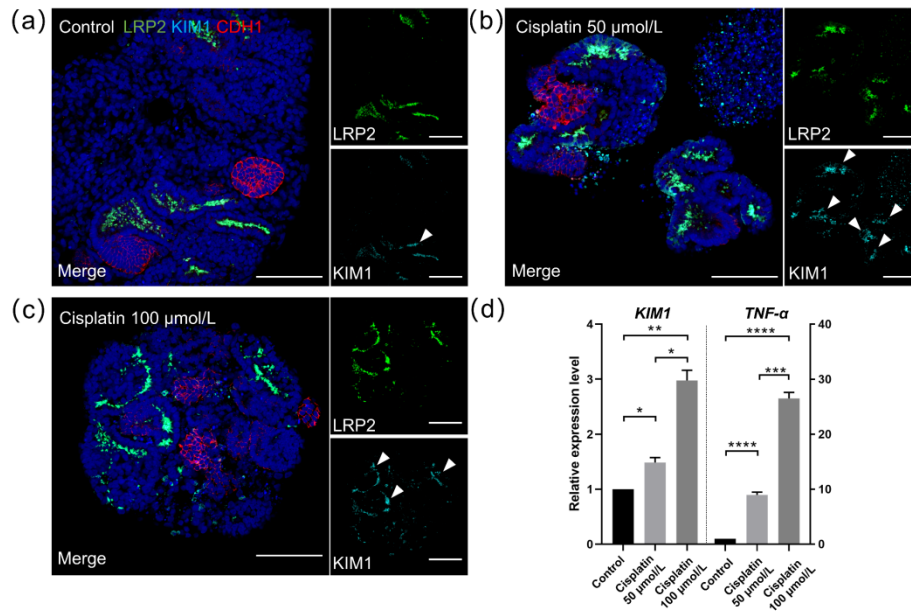


Fig. S5 Immunocytochemical and RT-qPCR analysis. (a–c) Immunofluorescence staining of organoids after cisplatin treatment using proximal tubule marker LRP2 (green), tubular injury marker KIM1 (cyan), and distal tubule marker CDH1 (red), then co-stained with DAPI (blue) in the merged channels. The white arrowheads denote the KIM1+ cells. (d) RT-qPCR analysis for the expression of *KIM1* and proinflammatory cytokine gene *TNF- α* in kidney organoids treated with cisplatin at indicated doses. The left and right y-axis represent the relative expression level of *KIM1* and *TNF- α* , respectively. Data are expressed as mean \pm SEM. (n=3). * $P < 0.05$, ** $P < 0.01$, *** $P < 0.001$, **** $P < 0.0001$. LRP2: lipoprotein receptor-related protein-2; KIM1: kidney injury molecule-1; CDH1: cadherin-1; DAPI: 4',6-diamidino-2-phenylindole. Scale bars, 100 μ m (a–c).

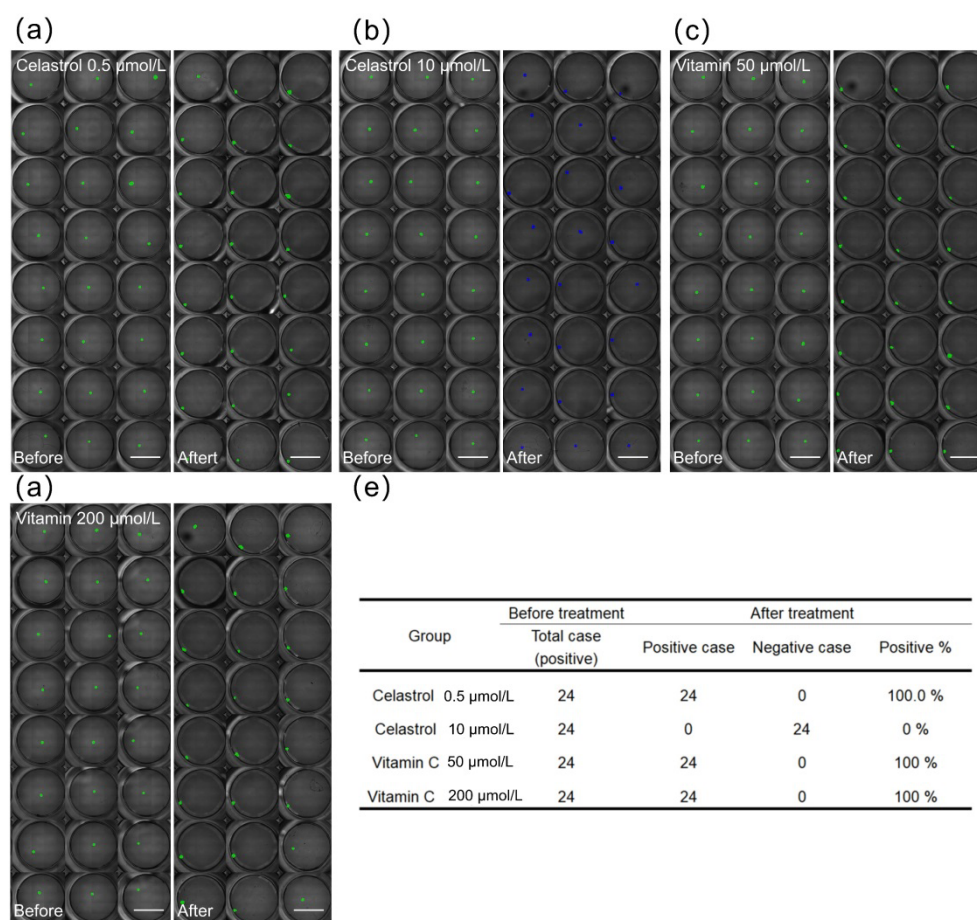


Fig. S6 “Read-on-ski” system performance of organoid-based drug screening in 96-well plates. (a–d) The detection of organoids before and after treatment with celastrol and vitamin C at indicated doses. Positive and negative case kidney organoids are marked as green and blue, respectively. (e) Detection of kidney organoids before and after treatment with different compounds. Scale bars, 5 mm (a–d).

Table S1 Number of kidney organoids before and after treatment with cisplatin at indicated doses in each category after detection by the “read-on-ski” system

Group	Positive cases		Negative cases		Adhesion cases		Total Cases	
	Before	After	Before	After	Before	After	Before	After
Control	218	91	28	25	41	86	287	202
Cisplatin 50 $\mu\text{mol/L}$	181	101	15	58	15	15	211	174
Cisplatin 100 $\mu\text{mol/L}$	215	8	19	123	15	35	249	166